Forecasting global aluminium flows to demonstrate the need for improved sorting and recycling methods

Peer-reviewed author version

Van den Eynde , S; Bracquene, E; Diaz-Romero, D; Zaplana, I; ENGELEN, Bart; Duflou, JR & Peeters, Jef (2022) Forecasting global aluminium flows to demonstrate the need for improved sorting and recycling methods. In: Waste management (Elmsford), 137 , p. 231 -240.

DOI: 10.1016/j.wasman.2021.11.019
Handle: http://hdl.handle.net/1942/37730

Forecasting Global Aluminium Flows to Demonstrate the Need for Improved Sorting and Recycling Methods

Simon Van den Eynde[1], Ellen Bracquené[1], Dillam Diaz-Romero[1,2], Isiah Zaplana[1], Bart Engelen[1,3], Joost R. Duflou[1,4], Jef R. Peeters[1]

Department of Mechanical Engineering - KU Leuven, Celestijnenlaan 300A, Box 2422, 3001 Leuven, Belgium[1]

PSI-EAVISE - KU Leuven, 2860 Sint-Katelijne-Waver, Belgium[2]

Technology Campus Diepenbeek - KU Leuven, Agoralaan Gebouw B, 3590 Diepenbeek, Belgium[3]

Member of Flanders Make[4]

Abstract

The probable emergence of a global aluminium scrap surplus in the coming decade is one of the main incentives for the aluminium recycling industry to invest in new methods and technologies to collect, sort and recycle aluminium scrap. However, due to the considerable uncertainty in the evolution of the global scrap surplus, it is difficult for policymakers and the recycling industry to accurately estimate the economic and environmental advantages of implementing enhanced sorting and recycling methods. The International Aluminium Institute (IAI) has developed a model to track and forecast the global flows of aluminium, but this model is not extensive enough to estimate the scrap surplus evolution. Therefore, this paper introduces an alloy series resolution to the supply and demand of aluminium in the IAI's global flow model and estimates the composition of the recovered scrap flows to improve the estimate of the technical potential of secondary alloy production. The estimated scrap surplus evolution is subjected to a sensitivity analysis, considering the most critical parameters, including the speed of electrification in the automotive sector, the recovered scrap's composition and the lifetime of aluminium products. In addition, the estimated

composition of the recovered aluminium scrap in the model is compared to composition measurements of alumimium scrap collected at a Belgian recycling facility as a means of validation. This study allows to estimate that the global aluminium scrap surplus will emerge soon and reach a size of 5.4 million tonnes by 2030 and 8.7 million tonnes by 2040, if currently adopted aluminium sorting and recycling methods are not improved.

Keywords: *Aluminium, Forecasting, Material Flow Analysis, Alloys, Scrap surplus*

1 Introduction

The demand for aluminium has been increasing drastically since 1950 due to the global population's growth and the improved standard of living (European Aluminium Association, 2021). To date, aluminium is the second most-produced metal, preceded only by steel. Aluminium is produced more than all other non-ferrous metals combined (Cullen and Allwood, 2013). In the last two decades, the demand for aluminium has grown faster than that for any other metal, increasing at a significantly faster rate than the global GDP (Fog, 2019). Its light weight, high strength, good corrosion resistance and high conductivity make aluminium an attractive choice for many products, including food packaging, car parts, airplane components and building features. The increased use of aluminium has led to significant weight reductions of components in the automotive and aerospace sector which have saved large amounts of fuel in the use phase of cars, trucks, and planes (European Aluminium Association, 2013). However, aluminium production itself has substantial environmental impact, in the form of toxicity, acidification, greenhouse gas emissions and resource depletion (Schlesinger, 2017; The Economist, 2007). In 2020, the primary production of aluminium was responsible for the emission of more than 1 billion metric tonnes of CO_2-equivalents, accounting for almost 2% of the global human-caused emissions in that year (Saevarsdottir et al., 2020; Van Heusden et al., 2020). In order to reduce the aluminium industry's environmental impact, companies and policymakers increasingly focus

on aluminium recycling as a potential solution, with as main driver the substantial difference in energy consumption: producing 1 kg of recycled aluminium requires on average 9.2 MJ, compared to 144.6 MJ for producing 1 kg of primary aluminium (Peng et al., 2019).

The European Aluminium Association (EAA), the organisation representing the European aluminium industry, forecasts a rise in the share of recycled aluminium in European end-use products from 26% in 2000 to 49% in 2050 (European Aluminium Association, 2019). In its "VISION 2050" report, the EAA explains that this is an ambitious but realistic evolution that will significantly contribute to the European decarbonisation efforts. However, most collected aluminium scrap today contains a mixture of different alloy types. As a result, different alloying elements and impurities are present in the scrap. Removing these elements metallurgically from the secondary aluminium is notoriously difficult (Nakajima et al., 2010). Therefore, most collected aluminium scrap is "downcycled" and used for the production of cast aluminium alloys, which have high tolerances for impurities (Paraskevas et al., 2015). A smaller share of the collected scrap is used to produce wrought aluminium alloys, which have much lower tolerances for alloying elements and impurities. To produce wrought alloys from mixed scrap, it needs to be diluted with large amounts of primary aluminium.

Although this downcycling practice has been a successful strategy because of the high demand for cast aluminium alloys for the production of combustion engines, this is expected to change with the electrification of the automotive industry. Due to this transition, the global demand for cast aluminium alloys will stagnate or is even expected to decline (BloombergNEF, 2019; Modaresi and Müller, 2012). Simultaneously, the amount of aluminium scrap collected from end-of-life products and the demand for wrought aluminium alloys will keep growing. Previous research has suggested that, if the current practice of systematic downcycling is maintained, the collected amount of aluminium scrap will soon exceed the capacity of wrought and cast alloy production to absorb the secondary aluminium.

As such, an amount of aluminium scrap would be collected for which there is no suitable application. This amount of aluminium scrap is commonly referred to as a scrap surplus. Hatayama et al. (2012) estimate the scrap surplus size at 6.1 million tonnes in 2030. Modaresi and Müller (2012) and Modaresi et al. (2014) expect a scrap surplus of 4.2 million tonnes in 2030 that will grow to a size of 14 million tonnes by 2050. However, they add that due to the uncertainty in their parameters, the scrap surplus's actual size could lie anywhere between 3.3 and 18.3 million tonnes in 2050.

Therefore, this paper estimates the evolution of the global scrap surplus by expanding the global flow model of the International Aluminium Institute (IAI). This model is a prominent tool in the aluminium industry that tracks and predicts the volumes of aluminium throughout the different life cycle stages. In this paper, an alloy series resolution is introduced in the supply and demand data of the IAI and the composition of the recovered scrap flows is estimated to improve the estimate of the technical potential of secondary alloy production. The estimated evolution of the global scrap surplus is also subjected to a sensitivity analysis, considering the most critical uncertain parameters that affect its growth. In addition, the estimated composition of the recovered aluminium scrap in the model is compared to composition measurements of aluminium scrap collected at a Belgian recycling facility as a means of validation. These measurements are performed using a handheld X-Ray Fluorescence (XRF) device.

2 Methodology

2.1 Demand for Aluminium Alloys

The IAI publishes annual data on the global flows of aluminium from different studies and surveys. Bertram et al. (2009) combined these data into a single model, which resulted in the first global flow model for aluminium, published in 2009. Ever since, the global aluminium

flow model of the IAI has been updated regularly (Bertram et al., 2017). Stakeholders in the aluminium industry often refer to the model, that is freely accessible on the website of the IAI (NTNU et al., 2020). Similar efforts to model and predict (global) flows of aluminium have been made by other researchers as well (Dai et al., 2019; Zhu et al., 2021).

Figure 2.1 is adapted from Bertram et al. (2017) and shows the structure of the IAI's global flow model. It models the flows of aluminium throughout the life cycle stages per region and then links all regions together. The global flow data of the IAI include the amounts of aluminium that flow to the manufacturing phase in the different industrial sectors since 1950, and projections are made for these flows until the year 2040. Because the IAI has access to extensive databases from reliable sources worldwide, the accuracy of their data is unparalleled. No other material industry has succeeded in quantitatively modelling global material flows with a similar level of accuracy (Bertram et al., 2009). However, the major drawback of the MFA model of the IAI is that the aluminium is treated as a single, uniform material that seems unaltered when it goes from one stage in the lifecycle to the next. However, in practice aluminium is mostly alloyed, and the aluminium material flows undergo significant compositional changes, especially in the end-of-life phase. Another significant drawback of the IAI's model is that it assumes that all collected aluminium scrap can be remelted into new alloys without verifying the allowable recycled content. Therefore, the IAI's model cannot predict a possible emergence of a scrap surplus. Furthermore, the authors chose to rely on projections of the EAA (European Aluminium Association, 2019) for the demand for aluminium between 2030 and 2040 instead of using the numbers of the IAI. The main difference is that the EAA forecasts a demand that keeps growing significantly up to 2040 while the IAI expects the demand to stagnate more between 2030 and 2040. Even though the methodology behind the projections of the EAA is not elaborately explained in the published report itself, the authors chose to use these numbers because they are the result of

more recent research and because they are probably more accurate, since they were specifically estimated by CRU, a market analysis firm specialised in metals, whereas the projections of the IAI are based on a relatively simple time series.

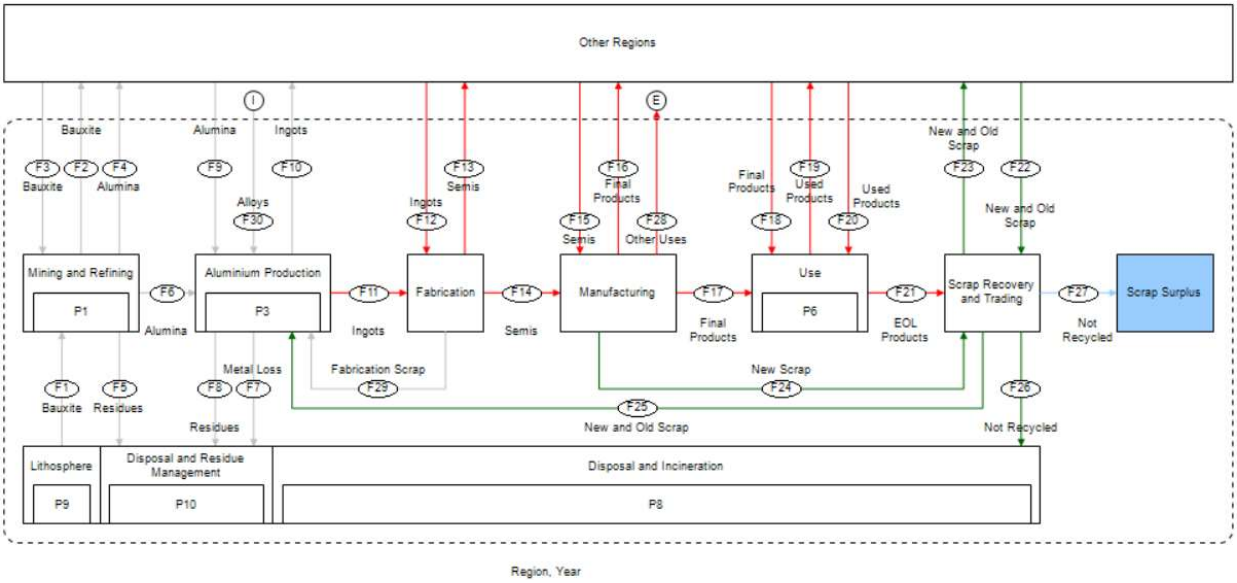

Figure 2.1: Additions to the global flow model of the International Aluminium Institute (red: alloy series resolution; green: composition estimate; blue estimate scrap surplus size), based on Bertram et al. (2017)

To overcome these shortcomings, the structural contributions of this paper to the global flow model of the IAI are threefold. Firstly, it introduces alloy series resolution into the modelled supply and demand of aluminium. The demand for aluminium ingots, semis, and final products, as well as the generation of aluminium EOL products, is modelled on an alloy level in this research, whereas the global flow model of the IAI only estimates the volumes of aluminium. The flows in red in Figure 2.1 (F11-21) are the ones for which the alloy series resolution is added. Secondly, whereas the global flow model of the IAI only estimates the total volumes of generated aluminium scrap, the presented research includes the elemental composition of the recovered aluminium scrap, based on the estimated amounts of alloys in recovered EOL products. The flows for which the elemental composition is calculated are indicated in green (F23-26). The global flow model of the IAI only estimates the volumes of generated aluminium scrap. Finally, the developed model estimates the size of the generated

scrap surplus, which is not considered at all in the global flow model of the IAI. This contribution is indicated in blue (F27). The remainder of the model is unchanged with respect to the original IAI model.

The alloy series resolution in the demand for aluminium is introduced by determining each aluminium alloy series' share in the annual aluminium demand per industrial sector. This demand (D_{SECTOR}^{SERIES}) is calculated by multiplying the total demand for aluminium in a sector (D_{SECTOR}), according to the data of the IAI, by the share of that alloy series in the demand of that sector (S_{SECTOR}^{SERIES}), as expressed in Formula 2.1. The annual shares of the alloy series in the total demand for aluminium per sector, considering evolutions in the demand over time, are determined by performing an extensive literature study, as detailed in Appendix 1, combining industry data, governmental data and data published by previous research on aluminium use for all 12 sectors that are defined by the IAI: (1) "Building & Construction", (2) "Transportation – Auto & Light Truck", (3) "Transportation – Aerospace", (4) "Transportation – Other", (5) "Packaging – Cans", (6) "Packaging – Other (Foil)", (7) "Machinery & Equipment", (8) "Electrical – Cable", (9) "Electrical – Other", (10) "Consumer Durables", (11) "Other (except Destructive Uses)", and (12) "Destructive Uses". **Error! Reference source not found.** in Appendix 2 illustrates the shares of the alloy series in the total demand for aluminium in the defined sectors for the year 2020 and indicates on which references the data are based.

$$D_{SECTOR}^{SERIES} = D_{SECTOR} \cdot S_{SECTOR}^{SERIES} \tag{2.1}$$

2.2 Scrap Generation

Secondary aluminium is sourced from "new scrap" and "old scrap". New scrap, also referred to as production scrap or pre-consumer scrap, is generated in the manufacturing phase due to process inefficiencies. Old scrap originates from end-of-life products. The annual amounts of

new and old scrap collected for recycling from each industrial sector are included in the IAI data. The developed model requires both the elemental composition of the collected scrap and the volumes of these scrap flows. In the model's calculations, the composition of the scrap is first determined on an alloy level and then converted to an elemental level.

For new scrap, it is assumed that the generated scrap in a certain year consists of the same alloys that entered the manufacturing phase that year. As such, the amount of new scrap from a specific alloy series that is generated in an industrial sector in a specific year ($A_{NEW}^{SERIES,SECTOR}$) can be calculated by multiplying the total amount of generated new scrap in the sector (A_{NEW}^{SECTOR}) with the share of the alloy series in the demand for aluminium in the sector (S_{SECTOR}^{SERIES}). The total amount of generated new scrap from a specific alloy series (A_{NEW}^{SERIES}) can be calculated by adding up the amounts of the different sectors. Dividing this number by the total amount of collected new scrap (A_{NEW}) gives the share of scrap from a certain alloy series in the total amount of collected new scrap (C_{NEW}^{SERIES}). These calculations are summarised below in Formulas 2.2 to 2.4. Calculating every alloy series' share leads to a complete alloy level composition of the collected new scrap. This alloy level composition still has to be converted to an elemental level composition.

$$A_{NEW}^{SERIES,SECTOR} = A_{NEW}^{SECTOR} \cdot S_{SECTOR}^{SERIES} \tag{2.2}$$

$$A_{NEW}^{SERIES} = \sum_{SECTOR} (A_{NEW}^{SECTOR} \cdot S_{SECTOR}^{SERIES}) \tag{2.3}$$

$$C_{NEW}^{SERIES} = A_{NEW}^{SERIES} / A_{NEW} \tag{2.4}$$

For old scrap, estimating which alloys can be expected in the collected scrap is more complex since most aluminium products have a much longer lifetime than one year. Therefore, the alloys collected from end-of-life products in a specific year are not identical to those that entered the use phase during that year. The average time aluminium remains “in stock” in the use phase is estimated by the IAI per sector and region. It varies from one year for packaging

to 60 years for aluminium in buildings (Bertram et al., 2017). For the developed MFA model, it is assumed that the alloy series in the scrap of a sector are present in the same proportions as the alloy series that entered the use phase one average lifetime ago for the products in that sector. This assumption does not allow to consider possible variations in the lifetime of the products within a sector. However, this approach still yields reasonable approximations since, in most sectors, the use of alloys in the manufacturing process changes only gradually during the products' average lifetime.

With this assumption, the amount of old scrap from a particular alloy series from a certain sector that is collected for recycling ($A_{OLD}^{SERIES,SECTOR}$) can be calculated similarly as for the new scrap (see Formula 2.5). A_{OLD}^{SECTOR} is the amount of old scrap from an industrial sector collected for recycling. Annual numbers for these scrap flows are included in the IAI data, as well as the amount of aluminium end-of-life scrap that is not collected for recycling. This scrap mostly ends up in landfills. The apostrophe in the symbol S'_{SECTOR}^{SERIES} stresses the time delay between the manufacturing phase and the end-of-life phase of the aluminium products in the sector, which must be considered.

The total amount of scrap from each alloy series in the collected old scrap from all sectors (A_{OLD}^{SERIES}) can be calculated by summing up the amounts from the different industrial sectors, as expressed in Formula 2.6. An exceptional flow in the developed MFA model is the collected aluminium scrap from used beverage cans (UBC). The researchers that contributed to the global flow model of the IAI indicate that scrap from UBC reaches cast houses mostly separately from casting scrap, extruded scrap, rolled scrap and other scrap from different sources (Bertram et al., 2017). Therefore, UBC recycling is modelled as a closed-loop system, separate from the remainder of the collected scrap. As such, the “Packaging – Cans” sector is not included in the summation of Formula 2.6. The amount of aluminium that has to

be produced for this sector with the "conventional" method is reduced by the amount of closed-loop recycled UBC. Formula 2.7 expresses how the concentration of the scrap from a particular alloy series in the total amount of collected old scrap (C_{OLD}^{SERIES}) is calculated. Calculating the concentration of every alloy series leads to a complete alloy level composition of the collected old scrap. As for the new scrap, this alloy level composition has to be converted to an elemental level composition.

$$A_{OLD}^{SERIES,SECTOR} = A_{OLD}^{SECTOR} \cdot S'^{SERIES}_{SECTOR} \tag{2.5}$$

$$A_{OLD}^{SERIES} = \sum_{SECTOR} (A_{OLD}^{SECTOR} \cdot S'^{SERIES}_{SECTOR}) \tag{2.6}$$

$$C_{OLD}^{SERIES} = A_{OLD}^{SERIES} / A_{OLD} \tag{2.7}$$

2.3 Conversion from alloy level composition to elemental composition

To convert the calculated alloy level composition of the new and old scrap to an elemental composition, it is necessary to know the approximate elemental composition of the different alloy series. However, the composition of an alloy series is not strictly specified. While all alloys within a series have the same main alloying element(s), there are still some differences in composition between specific alloys.

In order to come to a generalised elemental composition of each alloy series, the most popular alloys are selected to represent the average elemental composition of their alloy series. The selected alloys are listed in the first column of Table 2.1, below the alloy series they represent. Based on these alloys, the average concentrations of the alloying elements and impurities are determined for each wrought alloy series and the cast alloys. These concentrations are given in the "Average" rows of Table 2.1. Combining these concentrations with the calculated alloy level composition of the collected new and old scrap allows to calculate the composition of the collected scrap on an elemental level.

The concentration of an alloying element in the collected new or old scrap from a certain sector ($C_{SECTOR,NEW}^{ELEMENT}$) can be calculated with Formulas 2.8 and 2.9. The symbol $C_{SERIES}^{ELEMENT}$ stands for the values in the "Average" rows of Table 2.1. The mass of an alloying element in the total amount of collected scrap can be calculated with Formula 2.10. Dividing this value by the total mass of all collected scrap, except for the collected UBC, gives the concentration of the alloying element in the total amount of collected scrap (see Formula 2.11). Calculating the concentrations of all alloying elements and impurities gives a complete composition of the collected scrap on an elemental level.

$$C_{SECTOR,NEW}^{ELEMENT} = \sum_{SERIES} (0.01 \cdot C_{SERIES}^{ELEMENT} \cdot S_{SECTOR}^{SERIES}) \tag{2.8}$$

$$C_{SECTOR,OLD}^{ELEMENT} = \sum_{SERIES} (0.01 \cdot C_{SERIES}^{ELEMENT} \cdot S'^{SERIES}_{SECTOR}) \tag{2.9}$$

$$A_{ALL\ SCRAP}^{ELEMENT} = \sum_{SERIES} \left((A_{NEW}^{SERIES} + A_{OLD}^{SERIES}) \cdot 0.01 \cdot C_{SERIES}^{ELEMENT} \right) \tag{2.10}$$

$$C_{ALL\ SCRAP}^{ELEMENT} = A_{ALL\ SCRAP}^{ELEMENT} / (A_{NEW} + A_{OLD}) \tag{2.11}$$

2.4 Supply of Aluminium

Aluminium products are manufactured from a mixture of primary and secondary aluminium. Due to the presence of alloying elements and impurities in the collected scrap, the capacity of wrought alloys to absorb secondary aluminium is limited. The recycled content of the wrought alloy series (this is the allowable mass fraction of secondary aluminium in the mixture of primary and secondary aluminium used to produce wrought alloys) can be calculated based on the calculated composition of the collected scrap and the estimated tolerances for impurities of the wrought alloy series. Aluminium alloys have an allowable range of concentrations for alloying elements and impurities. The tolerance of an aluminium alloy for an element is defined here as the maximum allowable concentration of that element in the aluminium alloy. As for the average concentration, the tolerances of an alloy series are

not strictly specified. Therefore, the tolerance of an alloy series for an element is determined in this research by selecting the lowest tolerance for that element among the representative alloys listed in Table 2.1. The resulting tolerances ("Tol") of the wrought alloy series for the different alloying elements and impurities can be found in the last row of each alloy series in Table 2.1.

Table 2.1: Concentrations and Tolerances for Alloying Elements and Impurities of the Wrought Alloy Series and Cast Alloys based on (Aircraft Materials, 2020; AZO Materials 2005, 2013; MakeItFrom, 2020; Matweb, 2020)

Alloy series (representative alloys)	**Statistic**	**Cu (wt%)**	**Fe (wt%)**	**Mg (wt%)**	**Mn (wt%)**	**Si (wt%)**	**Zn (wt%)**	**Other (wt%)**
	Min	0	0	0	0	0	0	0
1000	Max	0.20	1.00	0.05	0.05	1.00	0.10	0.15
(1050, 1100, 1200)	Average	0.05	0.20	0.04	0.02	0.20	0.05	0.10
	Tol	0.05	0.40	0.05	0.05	0.25	0.05	0.06
	Min	3.80	0	0	0.30	0	0	0
2000	Max	5.00	1.00	1.80	1.20	1.20	0.25	0.15
(2014, 2024, 2025)	Average	4.50	0.20	1.00	0.50	0.60	0.10	0.10
	Tol	4.90	0.50	0.05	0.90	0.50	0.25	0.15
	Min	0	0	0.80	1.00	0	0	0
3000	Max	0.25	0.70	1.30	1.50	0.30	0.25	0.15
(3004)	Average	0.10	0.50	1.10	1.30	0.15	0.10	0.10
	Tol	0.25	0.70	1.30	1.50	0.30	0.25	0.15
	Min	0	0	0	0	4.50	0	0
4000	Max	0.30	0.80	0.05	0.05	6.00	0.10	0.15
(4043)	Average	0.10	0.20	0.03	0.03	5.20	0.05	0.10
	Tol	0.30	0.80	0.05	0.05	6.00	0.10	0.15
	Min	0	0	0.50	0	0	0	0
5000	Max	0.20	0.70	5.00	0.20	0.40	0.25	0.15
(5005, 5052, 5083)	Average	0.05	0.20	3.00	0.10	0.25	0.10	0.10
	Tol	0.10	0.35	1.10	0.10	0.25	0.10	0.15
	Min	0	0	0.45	0	0.20	0	0
6000	Max	0.40	0.70	1.20	1.00	1.30	0.25	0.15
(6061, 6063, 6082)	Average	0.20	0.30	1.10	0.30	0.70	0.10	0.10
	Tol	0.10	0.35	0.90	0.10	0.60	0.10	0.15
	Min	1.20	0	1.90	0	0	5.10	0
7000	Max	2.60	0.50	2.90	0.30	0.40	6.70	0.25
(7050, 7075, 7475)	Average	1.80	0.30	2.40	0.10	0.10	6.00	0.20
	Tol	1.90	0.12	2.60	0.06	0.10	6.10	0.15
	Min	0	0.40	0	0	0.03	0	0
8000	Max	0.05	1.00	0.05	0.05	0.15	0.10	0.15
(8176)	Average	0.05	0.70	0.05	0.05	0.10	0.05	0.10
	Tol	0.05	1.00	0.05	0.05	0.15	0.10	0.15
Cast alloys (319, 356, 380)	Average	2.50	0.60	0.30	0.30	7.10	1.20	0.30

A conservative specification of the tolerances is deliberately introduced to ensure that the allowable recycled content of the wrought alloy series is not overestimated. It should be

considered that old scrap is always contaminated to some extent with other materials, resulting from separation errors, imperfect liberation of laminated or shape included materials and unliberated joints. Previous research has demonstrated that aluminium output fractions in state-of-the-art recycling facilities consist for 98.11 wt% to 99.57 wt% of aluminium alloys, depending on the size to which the material is shredded (Soo et al., 2018). Similar results are achieved by manual sorting by well trained workers (Capuzzi and Timelli, 2018). According to Soo et al. (2018), the majority (0.23-0.96 wt%) of the contaminatons in aluminium scrap is of an organic nature and, depending on the size of the shredded material, 0.03 wt% up to 0.36% is iron and 0.13 wt% up to 0.26 wt% is copper. These contaminants come on top of the amount of iron and copper that is present in the form of alloying elements in the aluminium scrap. Increasing the estimated amount of iron and copper in the recovered scrap to take into account these contaminants would require extrapolating the data that were acquired by Soo et al. (2018). Since this approach would result in increased complexity of the model and introduce additional uncertainty, the authors instead opted to use a more conservative specification of the tolerances to ensure that the allowable recycled content of the wrought alloy series is not overestimated.

The limit that the presence of an alloying element imposes on the use of secondary aluminium to produce a wrought alloy series ($L_{SERIES}^{ELEMENT}$) is calculated by dividing the alloy series' tolerance for the element by the concentration of the element in the collected scrap (see Formula 2.12). The collected scrap is assumed to be a mix of both old and new scrap from all sectors. Each alloying element imposes a limit ($L_{SERIES}^{ELEMENT}$) on the use of secondary aluminium for the production of the wrought alloy series. The maximum recycled content of a wrought alloy series ($RC^{WR.SER}$) equals the lowest of the limits imposed by the different alloying elements in the scrap. This value indicates the mass percentage of secondary aluminium that can be used in the production of each wrought alloy series, and the

complement of this value is the mass percentage of primary aluminium necessary for diluting the scrap.

$$L_{SERIES}^{ELEMENT} = 0.01 \cdot T_{SERIES}^{ELEMENT} / C_{ALL\ SCRAP}^{ELEMENT} \quad (2.12)$$

Cast alloys have a very high capacity to absorb recycled material. Recycled aluminium can constitute 99.3 wt% or even more of the total aluminium mass in typical applications for cast alloys (Paraskevas et al., 2015). Modaresi et al. (2014) neglect the required aluminium for diluting cast alloys in their calculations to predict the emergence of a scrap surplus since this simplification only has a minimal impact on the overall result. For the same reason, this tiny fraction of primary aluminium that has to be added to recycled aluminium for the production of cast alloys is neglected in the developed model, and the maximum recycled content of cast alloys is, therefore, considered to be 100%.

The amount of secondary aluminium that can be used to produce new alloys is slightly lower than the amount of collected scrap due to premelting and melting losses during recycling. The IAI holds data on these losses involved in the recycling process of old and new scrap. According to the IAI, old scrap premelting recovery rates are consistently higher than 97% for any sector in any year, while old scrap melting recovery rates go as low as 85% for aluminium foil in the earlier years of the investigated time frame. For new scrap, premelting losses are neglected, and the melting recovery rate is estimated at 98% for each sector and each year. Considering these rates, the amounts of primary and secondary aluminium used in the production of the different alloy series and the scrap surplus size can be calculated.

The amount of secondary aluminium that can be used for the production of each wrought alloy series ($S_{SEC}^{WR.SER}$) is calculated by multiplying the global demand for the alloy series ($D^{WR.SER}$), as determined in Section 2.1, by its recycled content ($RC^{WR.SER}$). The amount of primary aluminium that flows to each wrought alloy series ($S_{PRI}^{WR.SER}$) is the difference

between the demand for the wrought alloy series ($D^{WR.SER}$) and the amount of recycled aluminium that flows to the alloy series ($S_{SEC}^{WR.SER}$). As long as the amount of generated aluminium scrap that is not used for wrought alloy production is smaller than the demand for cast alloys, there is no scrap surplus (SP). In this case, the scrap that is not used for wrought alloy production can be absorbed entirely by the cast alloys. The amount of primary aluminium used in the production of the cast alloys (S_{PRI}^{CAST}) is then equal to the difference between the demand for cast alloys (D^{CAST}) and the amount of secondary aluminium used in the production of cast alloys (S_{SEC}^{CAST}). However, if the amount of recycled aluminium exceeds the capacity of both wrought and cast alloys to absorb this material, there is no destination left for this flow. Then, the size of the scrap surplus is equal to the generated amount of scrap after melting and premelting losses (A'_{SEC}) minus the demand for cast alloys and the amount of secondary aluminium used in wrought alloy production. These calculations are summarised in Formulas 2.13 to 2.17. All the model calculations have been made in a Microsoft Excel Workbook and are visualised in the form of a Sankey diagram using the Python programming language and the FloWeaver library (Lupton and Allwood, 2017; Lupton, 2017).

$$S_{SEC}^{WR.SER} = RC^{WR.SER} \cdot D^{WR.SER} \tag{2.13}$$

$$S_{PRI}^{WR.SER} = D^{WR.SER} - S_{SEC}^{WR.SER} \tag{2.14}$$

$$S_{SEC}^{CAST} = \begin{cases} A'_{SEC} - \sum_{SERIES} S_{SEC}^{WR.SER} & if\ A'_{SEC} - \sum_{SERIES} S_{SEC}^{WR.SER} < D^{CAST} \\ D^{CAST} & if\ A'_{SEC} - \sum_{SERIES} S_{SEC}^{WR.SER} > D^{CAST} \end{cases} \tag{2.15}$$

$$S_{PRI}^{CAST} = \begin{cases} D^{CAST} - \left(A'_{SEC} - \sum_{SERIES} S_{SEC}^{WR.SER}\right) & if\ A'_{SEC} - \sum_{SERIES} S_{SEC}^{WR.SER} < D^{CAST} \\ 0 & if\ A'_{SEC} - \sum_{SERIES} S_{SEC}^{WR.SER} > D^{CAST} \end{cases} \tag{2.16}$$

$$SP = \begin{cases} 0 & if\ A'_{SEC} - \sum_{SERIES} S_{SEC}^{WR.SER} < D^{CAST} \\ A'_{SEC} - D^{CAST} - \sum_{SERIES} S_{SEC}^{WR.SER} & if\ A'_{SEC} - \sum_{SERIES} S_{SEC}^{WR.SER} > D^{CAST} \end{cases} \tag{2.17}$$

2.5 Aluminium Scrap Sampling

The demand for aluminium alloys and the composition of the collected aluminium scrap are calculated in the model based on data from literature. To be able to compare the literature data with the actual composition of aluminium scrap collected at recycling facilities, composition measurements have been conducted on aluminium scrap samples collected at a Belgian recycling facility. A batch of 275 aluminium scrap samples with a total mass of over 10 kg was collected from the so called “Twitch (40-120 mm)” fraction at the recycling facility of Galloo in Menen, Belgium. This fraction consists almost exclusively of aluminium scrap. The aluminium in the Twitch fraction of Galloo is separated from other materials in the treated end-of-life waste streams by magnetic separation, density separation, eddy current separation, and optical separation (Eggers et al., 2019). According to the representatives of Galloo, the aluminium in the Twitch fraction originates on average for 40% from construction waste, for 40% from automotive waste and for 20% from waste from consumer durables.

The composition of the collected samples was measured with a handheld XRF device (Thermo Scientific Niton XL2). Based on the XRF measurements, the 275 samples were divided in five categories related to their alloy type. The 1000 series, 3000 series, and cast alloys are three separate categories. The 2000, 4000, 7000, and 8000 series alloys are combined in the “Other Wrought” category since they are significantly less popular than the other series and barely encountered during the measurements. The alloys of the 5000 and 6000 series are bundled in one category due to the difficulty of distinguishing between these series with the used measuring method.

2.6 Method for sensitivity analysis

Predicting the composition of the global aluminium flows and the size of the scrap surplus involves considerable uncertainties. Since the evolution of the scrap surplus is estimated by expanding the IAI's global flow model, not only the uncertainties that arise from the assumptions in this paper have to be considered, but also the uncertain parameters within the IAI model. Two sources of uncertainty that are introduced in this paper and that have a particularly high influence on the scrap surplus growth are the changing demand for cast alloys in the automotive sector and the composition of the collected scrap. The estimated demand for cast alloys in the automotive sector in the presented MFA model relies on the projections of Modaresi et al. (2014). However, predictions for the future demand of cast alloys for cars and light trucks vary significantly, depending on the consulted source, due to the considerable uncertainty in the rate at which electric vehicles will gain market share in the automotive sector in the coming decades (Hatayama et al., 2012; Buchner et al., 2017). Furthermore, the most critical parameter within the global flow model of the IAI is the lifetime of the products in the different sectors. To show how the estimated evolution of the scrap surplus is affected by these different uncertainties in the data, a scenario-based sensitivity analysis is performed.

Seven alternative scenarios are investigated in addition to the baseline scenario. In the first alternative scenario ("slow electrification"), the share of cast alloys in the aluminium demand in the automotive sector diverges gradually from the share assumed in the baseline scenario between 2020 and 2040. In 2020, this share is still assumed the same as in the baseline scenario, but it linearly increases until 2040 when it is ten percentage points higher than in the baseline scenario. This increased demand for cast alloys corresponds to a situation in which the transition towards electric vehicles takes place slower than anticipated in the baseline scenario. In the second alternative scenario ("fast electrification"), the share of cast

alloys in the automotive sector's aluminium demand is gradually decreased from 2020 onwards until it is ten percentage points lower than in the baseline scenario in 2040. This scenario represents a faster than anticipated electrification in the automotive sector.

The third and fourth alternative scenarios illustrate the influence of the composition of the collected aluminium scrap. In the baseline scenario, the secondary scrap composition is calculated based on the average concentration of alloying elements in the wrought alloys, as presented in the "Average" rows of Table 2.1. In the third ("Min Alloys") and fourth ("Max Alloys") alternative scenarios, the secondary scrap composition is calculated based on the values in the "Min" and "Max" rows in Table 2.2, respectively. In the third alternative scenario, an alloying element's concentration in an alloy is assumed to be 0.01wt% when no lower limit is specified for the production of that alloy. This is a very low value, even for wrought alloys, and considered the minimum concentration of an alloying element in collected scrap since, in a realistic instance, the average concentration of alloying elements and impurities will never be exactly zero. This specification is important to avoid too unrealistic values in this scenario. These two scenarios also offer an idea about the magnitude of the change in the size of the scrap surplus that results from the presence of tramp elements in the collected aluminium scrap. According to Soo et al. (2018), the iron and copper impurities due to tramp elements account for 0.03wt% to 0.36wt% and 0.13wt% to 0.26wt% of the aluminium scrap, respectively. In the third and fourth alternative scenario, the considered deviations in the iron and copper content are slightly larger than these numbers. Therefore, the considered deviations in these scenarios cover the range of impurity concentrations that can be realistically expected in aluminium scrap.

The fifth alternative scenario ("Galloo") considers the results of the scrap measurements. Whereas in the baseline scenario, the alloy-level composition of the scrap from the sectors "Building & Construction", "Transportation – Auto & Light Truck", and "Consumer

Durables" is determined based on literature data, in this alternative scenario the compositions are adjusted so that they match the results of the scrap measurements. The estimated share of the 1000 series, 3000 series, and cast alloys in the recovered scrap is increased, while the share of 5000, 6000, and 7000 series alloys is decreased with respect to the literature data. The purpose of including this scenario is to demonstrate the sensitivity of the scrap surplus growth to the alloy-level composition of the collected old scrap.

To demonstrate the sensitivity of the scrap surplus evolution to the product lifetimes assumed in the IAI global flow model, a sixth and seventh alternative scenario have been developed. In the global flow model, global average lifetimes of aluminium products are estimated per sector (see Appendix 3). In the sixth scenario, these average lifetimes are reduced in a linear way with 10% between 2020 and 2040. In the seventh alternative scenario, the average lifetimes are reduced in a linear way by 20% between 2020 and 2040.

3 Results & Discussion

3.1 Limits to recycled content for wrought alloys

Table 3.1 shows the limit that each element in the collected aluminium scrap imposes on the recycled content of the different wrought alloy series ($L_{SERIES}^{ELEMENT}$) in 2020. The recycled content ($RC^{WR.SER}$), the most critical limit for each alloy series, is marked in yellow.

Table 3.1 Calculated Upper Limits for the Recycled Content of the Wrought Alloy Series in 2020

Element	1000	2000	3000	4000	5000	6000	7000	8000
Cu	5%	100%	26%	31%	10%	10%	100%	5%
Fe	100%	100%	100%	100%	93%	93%	32%	100%
Mg	4%	4%	100%	4%	100%	89%	100%	4%
Mn	17%	100%	100%	17%	34%	34%	20%	17%
Si	9%	19%	11%	100%	10%	23%	4%	5%
Zn	8%	42%	42%	16%	16%	16%	10%	16%
Other	36%	90%	90%	90%	90%	90%	90%	90%

3.2 Sankey diagram

Figure 3.1 shows the Sankey diagram for the calculated aluminium flows in 2030. Diagrams for 2035 and 2040 are included in Appendix 4. In the Sankey diagram, the nodes are ordered according to the different lifecycle stages, and the colors indicate the alloy series or the type of aluminium that flows between the nodes. The scrap from UBC is recycled in a closed-loop recycling scheme, in contrast to the aluminium flows for the other end-of-life products. The scrap surplus is represented as a flow that starts in the supply phase, which cannot be connected to the manufacturing phase.

According to the model's calculations, the scrap surplus would constitute 11.4% of all collected aluminium scrap in 2030. This would mean that in 2030, only 88.6% of all collected and processed aluminium scrap could be used for the production of new wrought and cast alloys. By 2040, this share is estimated to decline to 84.0%. In such situation, the use of primary aluminium would continue to grow despite the abundant availability of aluminium scrap.

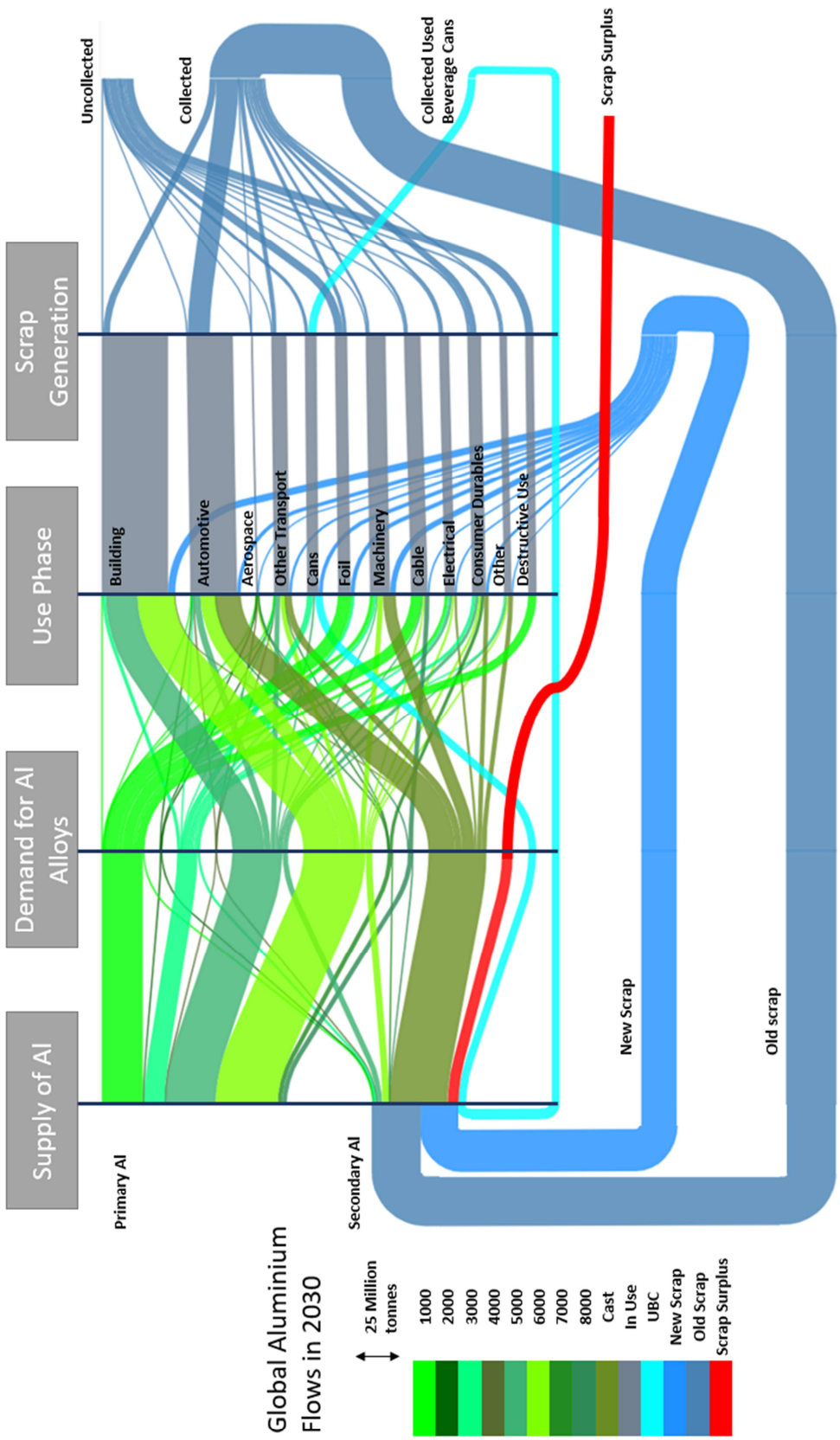

Figure 3.1: Sankey diagram representing the global aluminium flows in 2030, shades of green represent the alloy series (1000-8000 + cast), data in Appendix 5

3.3 Composition Measurements

Figure 3.2 shows the measured shares of the different alloy series in the set of aluminium (Twitch) scrap samples collected at Galloo, as well as the model's prediction for the composition of old scrap collected in 2020 from a mix of 40% scrap from construction, 40% automotive scrap and 20% scrap from consumer durables. The measured share of cast alloys in the Twitch fraction is relatively close to the estimated share. Among the wrought alloys, there are significant differences between the measured and estimated shares of the different alloy series. There are multiple explanations for these differences. First of all, it could be that the gathered sample does not exactly reflect the average composition of the Twitch fraction over the course of one year. The assumed origins of the measured scrap (40% construction, 40% automotive, and 20% consumer durables) are a company estimate of yearly averages. However, the composition of the scrap variates significantly throughout the year. Another important consideration is that the global average composition of a mix of old scrap is compared with the composition of the scrap at a local Belgian recycling facility. Since there are regional differences in the use of alloys for the production of aluminium products, it is not unexpected that the scrap collected in Belgium has a slightly different composition than the global average. The importance of an accurate estimate of the collected scrap's alloy-level composition for estimating the growth of the scrap surplus is shown in the sensitivity analysis in the next section.

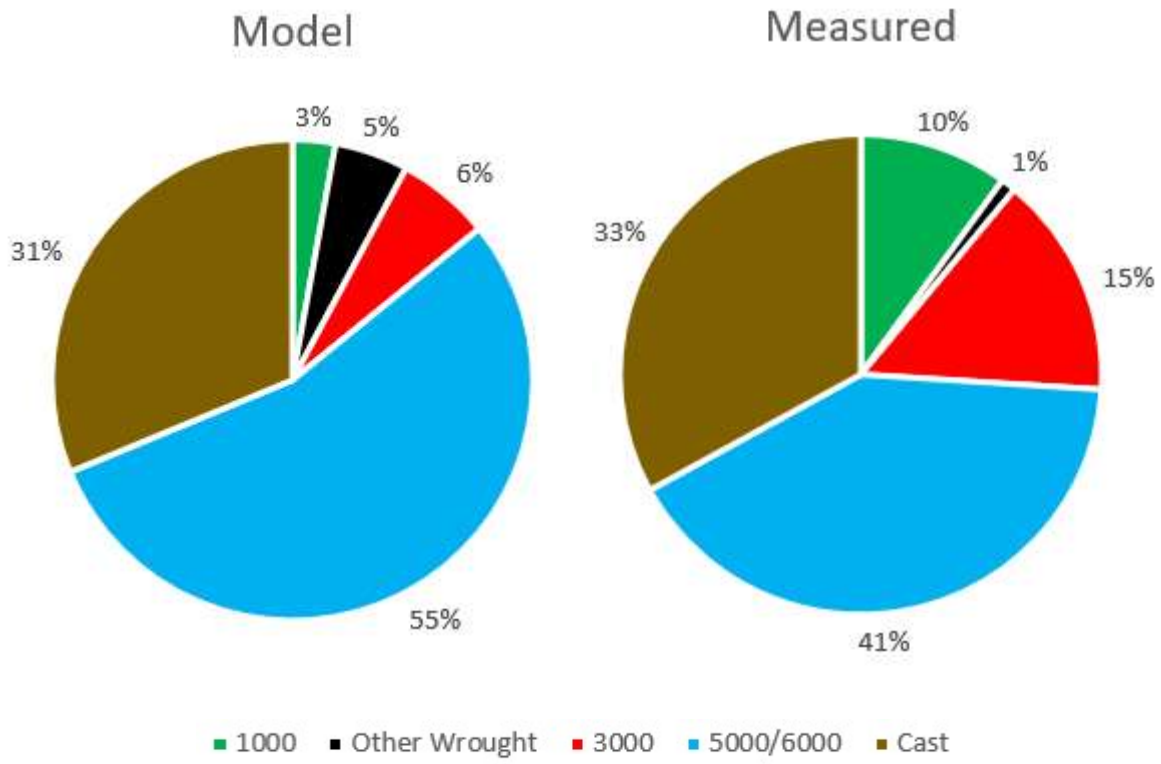

Figure 3.2: Alloy-level composition of collected scrap: Predicted by Model and Measured

3.4 Scenario-based sensitivity analysis for the evolution of the scrap surplus

Error! Reference source not found. shows the estimated evolution of the global scrap surplus between 2020 and 2040. In this figure, the baseline scenario of the predicted evolution is compared to seven other scenarios. These scenarios demonstrate the sensitivity of the scrap surplus's growth to the most important sources of uncertainty in the model. According to the calculations in the baseline scenario, a small global scrap surplus of 0.5 million tonnes first surfaced for one year in 2009, the year that the global economy contracted by almost 2% (The World Bank, 2021). In this year of recession, the London Metal Exchange suffered significant financial losses when its stock of aluminium increased by 152% in one year to 2.34 million tonnes (Salazar and McNutt, 2010). However, it is difficult to prove the scrap surplus's contribution to this incident since the most significant part of these stocks was probably the result of the overproduction of primary aluminium, as the sudden collapse in demand took many aluminium producers by surprise. Starting from 2023, an annual global

467 scrap surplus is predicted to arise and to continue to grow quickly to 5.4 million tonnes of
468 aluminium in 2030 and then to around 8.7 million tonnes in 2040. This prediction is
469 relatively close to what other researchers have predicted (Hatayama et al., 2008, 2012;
470 Modaresi and Müller, 2012; Modaresi et al., 2014). There is a kink in the scrap surplus
471 evolution in the year 2030, due to the decrease in the annual growth rate of the demand for
472 aluminium that is expected by the EAA. As a consequence, the generated amount of new
473 scrap and the amount of old scrap from products with very short lifetimes increase less
474 rapidly.

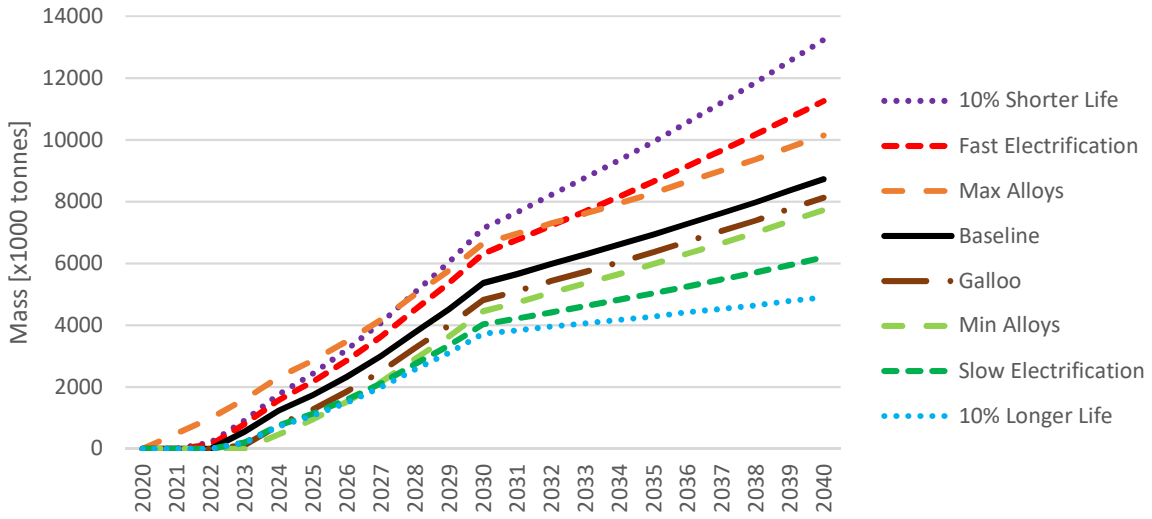

Figure 3.3: Sensitivity analysis for the evolution of the annual global aluminium scrap surplus, data in Appendix 5

475 Figure 3.3 shows that both the demand for cast alloys in the automotive sector and the
476 amount of alloying elements in the collected scrap have a significant influence on the scrap
477 surplus growth. The "Galloo" scenario lies relatively close to the baseline scenario, even
478 though there are significant differences between the measured alloy-level composition of the
479 collected scrap at Galloo and the alloy-level composition predicted from literature data.
480 Figure 3.2 showed that, especially among the wrought alloys, the predicted and measured

481 composition differed somewhat, while the shares of the cast alloys were very similar. The
482 fact that the "Galloo" scenario lies closer to the baseline scenario than the other alternative
483 scenarios indicates therefore that, for predicting the evolution of the scrap surplus, it is most
484 important to accurately determine the demand for cast alloys and the amount of cast alloys in
485 the collected scrap. Relatively small deviations in the shares of the wrought alloy series in the
486 composition of the scrap affect the scrap surplus much less. This is because the compositional
487 differences between the most popular wrought alloy series are much smaller than the
488 compositional difference between wrought and cast alloys in general.

489 The lifetime of the aluminium products also has a major influence on the evolution of the
490 scrap surplus. A linear decrease of 10% between 2020 and 2040 in the aluminium product
491 lifetimes adds 4.5 million tonnes to the global scrap surplus by 2040 with respect to the
492 baseline scenario. A linear increase of 10% in the product lifetimes between 2020 and 2040
493 leads to a 3.8 million tonnes decrease in the size of the annual global scrap surplus by 2040.
494 These results show that if the lifetime of aluminium products would decrease more rapidly
495 than expected, the scrap surplus would grow even faster. Such trend is not unthinkable, since
496 according to the IAI the average lifetime of aluminium products in the automotive sector is
497 already significantly below average (20 years) in regions such as Europe and North-America
498 (15 years), and Japan and the Middle-East (12 years). In China, the estimated lifetime of
499 aluminium products in the building sector is as short as 30 years, compared to a global
500 average of 50 years (Bertram et al., 2017). Furthermore, it should be considered that future
501 initiatives promoting the renovation of buildings and the replacement of older vehicles with
502 higher emissions for the sake of the environment could even further decrease the average
503 functional lifetime of aluminium products. Finally, it is also important to consider that the
504 mentioned sources of uncertainty can be combined. For example, a faster electrification of
505 the automotive sector could occur simultaneously as a decrease in the functional lifetime of

aluminium products. In that case, the scrap surplus would be even higher than in the documented scenarios.

The economic consequences of the Covid-19 (C19) pandemic have added another source of uncertainty to the estimate of the scrap surplus evolution. The demand forecasts used as input for the developed model are based on pre-C19 studies. 85% of the stakeholders interviewed by the IAI believe that the demand for aluminium will rebound to these pre-C19 levels by the end of 2021 (CM Group, 2020). Therefore, the authors expect that the C19 pandemic will have only a limited effect on the presented estimate beyond 2022. In any case, only the input data of the developed model have to be updated to compute a new estimate based on information gathered after the outbreak of C19.

Since the results of the model developed in this paper, as well as the results from other researchers, indicate that the emergence of a scrap surplus is imminent, the authors recommend that the IAI adopts a more thorough methodology for its global aluminium flow model. While it is already highly informative in its current form, it lacks the level of detail needed to estimate the scrap surplus evolution and the demand for specific alloys. The methodology, data, and results presented in this paper provide a possible starting point for the IAI to refine its global flow model.

4 Conclusions and future work

The presented research demonstrates that an aluminium scrap surplus will emerge in the coming decade if the aluminium recycling industry does not adopt enhanced sorting systems or improved recycling strategies. The developed MFA model estimates that a scrap surplus will emerge in the coming years and that its size will grow to 5.4 million tonnes in 2030 and to 8.7 million tonnes in 2040. Without countermeasures, the inability to recycle this amount of aluminium scrap will necessitate an additional increase in primary aluminium production,

which has a highly negative economic and environmental impact. The scenario-based sensitivity analysis shows that the evolution of the scrap surplus strongly depends on both the demand for cast alloys and the composition of the collected scrap. Composition measurements have been conducted on old scrap collected by a large Belgian recycling facility. The results are used in the sensitivity analysis to demonstrate how the estimated evolution of the scrap surplus is impacted by small deviations in the shares of the wrought alloy series in the collected aluminium scrap.

The level of detail of the IAI's global aluminium flow model could be increased by adopting the presented methodology. The relevance of tracking and estimating the global aluminium flows at alloy series level will only increase in the near future, as the aluminium industry will adapt the current methods of sorting and recycling aluminium scrap to increase the recycled content of wrought aluminium products. In future work, several methods to enhance current sorting and recycling practices will be investigated. Promising strategies to increase the recycled content of aluminium products are closed-loop recycling of aluminium products, separating old scrap from new scrap, and enhanced alloy-based sorting. The authors will investigate the benefits of separately processing waste streams of different sectors and the use of LIBS (Laser Induced Breakdown Spectroscopy) in combination with computer vision to sort old aluminium scrap at alloy series level. The extent to which these technologies can mitigate the growth of the global aluminium scrap surplus remains an important question, which the authors will also assess in future work, starting from the results of this paper.

5 Acknowledgements

This work has received funding from the European Institute of Innovation and Technology (EIT), a body of the European Union, under the Horizon 2020, the EU Framework

Programme for Research and Innovation in the AUtomatic SOrting of mixed scrap Metals (AUSOM) project (project number 19294, https://www.ausomproject.eu/).

Bibliography

Aircraft Materials, 2020. Alloy 4043/ Aluminium Welding Alloy 4043. https://www.aircraftmaterials.com/data/weld/4043.html (accessed: Apr. 09, 2021).

Allwood, J.M., Cullen, J.M., 2012. Sustainable Materials - with both eyes open : Future Buildings, Vehicles, Products and Equipment - Made Efficiently and Made with Less New Material, 1st ed. Cambridge, United Kingdom. https://www.bookdepository.com/Sustainable-Materials-with-both-eyes-open-Julian-Allwood/9781906860073 (accessed: Apr. 09, 2021)

Auxier, G.W., 1953. Aluminum and magnesium : history of the Aluminum and Magnesium Division of the National Production Authority. Washington, DC, USA: U.S. Dept. of Commerce, National Production Authority. https://catalog.hathitrust.org/Record/102381795 (accessed: Apr. 09, 2021)

Avallone, E.A., Baumeister, T., Sadegh, A.M., 2006. Marks' standard handbook for mechanical engineers, 11th ed. McGraw-Hill Professional Pub. https://www.abebooks.com/9780071428675/Marks-Standard-Handbook-Mechanical-Engineers-0071428674/plp (accessed: Apr. 09, 2021)

AZO Materials, 2005. Aluminium Alloys - Aluminium 5083 Properties, Fabrication and Applications. https://www.azom.com/article.aspx?ArticleID=2804 (accessed: Apr. 09, 2021)

AZO Materials, 2013. Aluminum 8176 Alloy (UNS A98176). https://www.azom.com/article.aspx?ArticleID=8788 (accessed: Apr. 09, 2021).

Belan, J., Vaško, A., Kuchariková, L., 2018. A brief overview and metallography for commonly used materials in aero jet engine construction. Production Engineering Archives, vol. 17, pp. 8–13. https://doi.org/10.30657/pea.2017.17.02

Bertram, M., Martchek, K.J., Rombach, G., 2009. Material Flow Analysis in the Aluminum Industry. Journal of industrial ecology, vol. 13, no. 5, pp. 650–654. https://doi.org/10.1111/j.1530-9290.2009.00158.x.

Bertram, M., Ramkumar, S., Rechberger, H., Rombach, G., Bayliss, C., Martchek, K.J., Müller, D.B., Liu, G., 2017. A regionally-linked, dynamic material flow modelling tool for rolled, extruded and cast aluminium products. Resources, conservation and recycling, vol. 125, pp. 48–69. https://doi.org/10.1016/j.resconrec.2017.05.014.

BloombergNEF, 2019. Electric Vehicle Outlook 2019. https://about.bnef.com/electric-vehicle-outlook/#toc-viewreport (accessed: Apr. 07, 2020)

Buchner, H., Laner, D., Rechberger, H., Fellner, J., 2017. Potential recycling constraints due to future supply and demand of wrought and cast Al scrap - A closed system perspective on Austria. Resources, conservation and recycling, vol. 122, pp. 135–142. https://doi.org/10.1016/j.resconrec.2017.01.014.

Campbell, F.C., 2006. Manufacturing Technology for Aerospace Structural Materials, 1st ed. Oxford, United Kingdom, 2006. https://doi.org/10.1016/B978-1-85617-495-4.X5000-8.

Capuzzi, S., Timelli, G., 2018. Preparation and Melting of Scrap in Aluminum Recycling: A Review. Metals - Open Access Metallurgy Journal, vol. 8. http://dx.doi.org/10.3390/met8040249

Chen, G., Wang, X., Wang, J., Liu, J., Zhang, T., Tang, W., 2012. Damage investigation of the aged aluminium cable steel reinforced (ACSR) conductors in a high-voltage transmission line. Engineering failure analysis, vol. 19, no. 1, pp. 13–21. https://doi.org/10.1016/j.engfailanal.2011.09.002.

Christel, H., 2006. Aluminum Building Wire Installation and Terminations. IAEI NEWS, pp. 78–85.

https://aluminum.org/sites/default/files/Aluminum%20Building%20Wire%20Installation %20&%20Terminations.pdf (accessed: Jun. 06, 2021)

CM Group, 2020. An Initial Assessment of the Impact of the Covid-19 Pandemic on Global Aluminium Demand. IAI. https://www.world-aluminium.org/media/filer_public/2020/05/28/initial_assessment_of_the_impact_of_the_covid-19_on_global_al_demand_.pdf (accessed: Apr. 28, 2021)

Cullen, J.M., Allwood, J.M., 2013. Mapping the Global Flow of Aluminum: From Liquid Aluminum to End-Use Goods. Environmental science & technology, vol. 47, no. 7, pp. 3057–3064. https://doi.org/10.1021/es304256s.

Dai, M., Wang, P., Chen, W., Liu, G., 2019. Scenario analysis of China's aluminum cycle reveals the coming scrap age and the end of primary aluminum boom. J ournal of Cleaner Production, vol 226, pp. 793-804. https://doi.org/10.1016/j.jclepro.2019.04.029.

Das, S.K., Green, J.A.S., Kaufman, J.G., Emadi, D., Mahfoud, M., 2010. Aluminum recycling—An integrated, industrywide approach. JOM, vol. 62, no. 2, pp. 23–26. https://doi.org/10.1007/s11837-010-0026-6.

Djukanovic, G., 2016. Aluminium alloys in shipbuilding – a fast growing trend. Aluminium Insider. https://aluminiuminsider.com/aluminium-alloys-in-shipbuilding-a-fast-growing-trend/ (accessed: Apr. 09, 2021)

Djukanovic, G., 2017. Aluminium use in the production of trains steams ahead. Aluminium Insider. https://aluminiuminsider.com/aluminium-use-production-trains-steams-ahead/#:~:text=Made%20in%20China%20%E2%80%93%20the%20high,speed%20of%20380%20km%2Fhr (accessed: Apr. 09, 2021).

Ducker Worldwide, 2011. Aluminum in 2012 North American Light Vehicles. Ducker Worldwide, Troy, Michigan, USA. http://www.drivealuminum.org/wp-

content/uploads/2017/05/2012_Aluminum-in-2012-North-American-Light-Vehicles.pdf (accessed: Apr. 09, 2021)

Ducker Worldwide, 2012. EAA Aluminium penetration in cars - Final Report. Ducker Worldwide, Troy, Michigan, USA. https://www.european-aluminium.eu/media/1308/eaa-aluminium-penetration-in-cars_final-report-public-version.pdf (accessed: Apr. 09, 2021)

Ducker Worldwide, 2017. Aluminum content in North American light vehicles 2016 to 2028. Ducker Worldwide, Troy, Michigan, USA. http://www.drivealuminum.org/wp-content/uploads/2017/10/Ducker-Public_FINAL.pdf (accessed: Apr. 09, 2021)

Eggers, A., Peeters, J.R., Waignein, L., Noppe, B., Dewulf, W., Vanierschot M., 2019. Development of a computational fluid dynamics model of an industrial scale dense medium drum separator. Engineering Applications of Computational Fluid Mechanics, vol. 13, no. 1, pp. 1001–1012. https://doi.org/10.1080/19942060.2019.1663559.

European Aluminium Association, 2013. Aluminium in Cars - Unlocking the light-weighting potential. https://european-aluminium.eu/media/1326/aluminium-in-cars-unlocking-the-lightweighting-potential.pdf (accessed: Apr. 07, 2021)

European Aluminium Association, 2015. The Aluminium Automotive Manual. https://www.european-aluminium.eu/resource-hub/aluminium-automotive-manual/ (accessed: Apr. 09, 2021)

European Aluminium Association, 2019. VISION 2050: European Aluminium's Contribution to the EU's Mid-Century Low-Carbon Roadmap. https://www.european-aluminium.eu/media/2552/sample_executive-summary-vision-2050_web_pages_20190408.pdf (accessed: Apr. 07, 2021)

Fog, K., 2019. Hydro Market Outlook. Norsk Hydro. https://www.hydro.com/Document/Index?name=Market%20outlook%20by%20Senior%

20Vice%20President%20and%20Head%20of%20Corporate%20Strategy%20%26%20Analysis%20Kathrine%20Fog&id=7873 (accessed: Apr. 07, 2021)

Hannula, J., Godinho, J.R.A., Llamas, A.A., Luukkanen, S., Reuter, M.A., 2020. Simulation-Based Exergy and LCA Analysis of Aluminum Recycling: Linking Predictive Physical Separation and Re-melting Process Models with Specific Alloy Production. Journal of Sustainable Metallurgy, vol. 6, no. 1, pp. 174–189. https://doi.org/10.1007/s40831-020-00267-6.

Hatayama, H., Daigo, I., Matsuno, Y., Adachi, Y., 2008. Assessment of Recycling Potential of Aluminium in Japan, the United States, Europe and China. Nihon Kinzoku Gakkai shi, vol. 72, no. 10, pp. 812–818. https://doi.org/10.2320/jinstmet.72.812.

Hatayama, H., Daigo, I., Matsuno, Y., Adachi, Y., 2012. Evolution of aluminum recycling initiated by the introduction of next-generation vehicles and scrap sorting technology. Resources, conservation and recycling, vol. 66, pp. 8–14. https://doi.org/10.1016/j.resconrec.2012.06.006.

Hatayama, H., Yamada, H., Daigo, I., Matsuno, Y., Adachi, Y., 2006. Dynamic Substance Flow Analysis of Aluminum and Its Alloying Elements. Nihon Kinzoku Gakkai shi, vol. 70, no. 12, pp. 975–980. https://doi.org/10.2320/jinstmet.70.975.

Kinsey, B., Wu, X., 2011. Tailor Welded Blanks for Advanced Manufacturing, 1st ed. Woodhead Publishing, 2011. https://www.elsevier.com/books/tailor-welded-blanks-for-advanced-manufacturing/kinsey/978-1-84569-704-4 (accessed: Apr. 09, 2021)

Lamifil, 2019. Specialty wires. https://lamifil.be/wp-content/uploads/2016/04/04-10-2019-specialities-brochure-lr.pdf (accessed: Apr. 09, 2021)

Lamifil, 2020. Aluminium alloys - Lamifil. https://lamifil.be/products/aluminium-alloys/ (accessed: Apr. 09, 2020)

Lupton, R.C., 2017. *ricklupton/sankeyview: v1.1.7*. Cambridge, United Kingdom. https://github.com/ricklupton/floweaver (accessed: Apr. 09, 2021)

Lupton, R.C., Allwood, J.M., 2017. Hybrid Sankey diagrams: Visual analysis of multidimensional data for understanding resource use. Resources, conservation and recycling, vol. 124, pp. 141–151. https://doi.org/10.1016/j.resconrec.2017.05.002.

MakeItFrom, 2020. Aluminum Alloys :: MakeItFrom.com. https://www.makeitfrom.com/material-group/Aluminum-Alloy (accessed: Apr. 09, 2021).

Matweb, 2020. Aluminum 4043-H18. http://www.matweb.com/search/datasheet_print.aspx?matguid=2541bb0127b34c7294612c77393ead8c (accessed: Apr. 09, 2021)

Modaresi, R., Lovik, A.N., Müller, D.B., 2014. Component- and Alloy-Specific Modeling for Evaluating Aluminum Recycling Strategies for Vehicles. JOM, vol. 66, no. 11, pp. 2262–2271. https://doi.org/10.1007/s11837-014-0900-8.

Modaresi, R., Müller, D.B., 2012. The Role of Automobiles for the Future of Aluminum Recycling. Environmental science & technology, vol. 46, no. 16, pp. 8587–8594. https://doi.org/10.1021/es300648w.

Nakajima, K., Takeda, O., Miki, T., Matsubae, K., Nakamura, S., Nagasaka, T., 2010. Thermodynamic Analysis of Contamination by Alloying Elements in Aluminum Recycling. Environmental science & technology, vol. 44, no. 14, pp. 5594–5600. https://doi.org/10.1021/es9038769.

NTNU, International Aluminium Institute, TruthStudio, Davies, J., 2020. Global Aluminium Cycle. IAI. https://alucycle.world-aluminium.org/public-access/#global (accessed: Apr. 08, 2021)

Paraskevas, D., Kellens, K., Dewulf, W., Duflou, J.R., 2015. Environmental modelling of aluminium recycling: a Life Cycle Assessment tool for sustainable metal management. Journal of Cleaner Production, vol. 105, pp. 357–370. https://doi.org/10.1016/j.jclepro.2014.09.102.

Peng, T., Ou, X., Yan, X., Wang, G., 2019. Life-cycle analysis of energy consumption and GHG emissions of aluminium production in China. Energy Procedia, vol. 158, pp. 3937-3943. https://doi.org/10.1016/j.egypro.2019.01.849.

Prasad, N.E., Wanhill, R.J.H., 2016. Aerospace Materials and Material Technologies: Volume 1: Aerospace Materials. Singapore: Singapore: Springer Singapore Pte. Limited. https://link-springer-com.kuleuven.ezproxy.kuleuven.be/book/10.1007%2F978-981-10-2134-3 (accessed: Apr. 09, 2021)

Saevarsdottir, G., Kvande, H., Welch, B.J., 2020. Aluminum Production in the Times of Climate Change: The Global Challenge to Reduce the Carbon Footprint and Prevent Carbon Leakage. JOM, vol. 72, no. 1, pp. 296–308. https://doi.org/10.1007/s11837-019-03918-6.

Salazar, K., McNutt, M.K., 2010. Minerals Yearbook - Metals and Minerals 2010, vol. 1. Eatsern Region, Reston, Va., USA: Department of the interior. Bureau of mines.

Schlesinger, M.E., 2017. Aluminum Recycling, 2nd ed. CRC Press. https://www.routledge.com/Aluminum-Recycling/Schlesinger/p/book/9781138073043 (accessed: Apr. 07, 2021)

Soo, V.K., Peeters, J., Paraskevas, D., Compston, P., Doolan, M., Duflou, J.R., 2018. Sustainable aluminium recycling of end-of-life products: A joining techniques perspective. Journal of Cleaner Production, vol. 178, pp. 119-132. https://doi.org/10.1016/j.jclepro.2017.12.235.

Southwire, 2020. Products | Southwire Overhead Transmission. https://overheadtransmission.southwire.com/products/ (Accessed: Apr. 09, 2020)

The Aluminum Association, 1989. Aluminum Electrical Conductor Handbook, 3rd ed. Washington, DC, USA: Aluminum Association. https://www.aluminum.org/sites/default/files/Aluminum%20Electrical%20Conductor%20Handbook.pdf (accessed: Jun. 06, 2021)

The Economist, 2007. The price of virtue. https://www.economist.com/leaders/2007/06/07/the-price-of-virtue (accessed: Apr. 07, 2021)

The World Bank, 2021. GDP growth (annual %) | Data. https://data.worldbank.org/indicator/ny.gdp.mktp.kd.zg (accessed: Apr. 09, 2021).

Van Heusden, R., Morrison, H., Puleo M., 2020. Why addressing the aluminium industry's carbon footprint is key to climate action, World Economic Forum. https://www.weforum.org/agenda/2020/11/the-aluminium-industry-s-carbon-footprint-is-higher-than-most-consumers-expect-heres-what-we-must-do-next/ (accessed: Apr. 07, 2021)

Zhu, Y., Cooper, D.R., 2019. An Optimal Reverse Material Supply Chain for U.S. Aluminum Scrap. Procedia CIRP, vol. 80, pp. 677–682. https://doi.org/10.1016/j.procir.2019.01.065.

Zhu, Y., Chappuis, L.B., De Kleine, R., Kim, H.C., Wallington, T.,J., Luckey, G., Cooper, D.R., 2021. The coming wave of aluminum sheet scrap from vehicle recycling in the United States. Resources, Conservation and Recycling, vol. 164. https://doi.org/10.1016/j.resconrec.2020.105208.